JACS
JOURNAL OF THE AMERICAN CHEMICAL SOCIETY

pubs.acs.org/JACS

Article

Solvent Organization and Rate Regulation of a Menshutkin Reaction by Oriented External Electric Fields are Revealed by Combined MD and QM/MM Calculations

Kshatresh Dutta Dubey,*[,‖] Thijs Stuyver,*[,‖] Surajit Kalita, and Sason Shaik*

Cite This: J. Am. Chem. Soc. 2020, 142, 9955−9965

Read Online

ACCESS | Metrics & More | Article Recommendations | Supporting Information

ABSTRACT: When and how do external electric fields (EEFs) lead to catalysis in the presence of a (polar or nonpolar) solvent? This is the question that is addressed here using a combination of molecular dynamics (MD) simulations, quantum mechanical/molecular mechanical calculations with EEF, and quantum mechanical/(local) electric field calculations. The paper focuses on a model reaction, the Menshutkin reaction between CH_3I and pyridine in three solvents of varying polarity. Using MD simulations, we find that the EEF causes the solvent to undergo organization; *the solvent molecules gradually align with the applied field as the field strength increases*. The collective orientation of the solvent molecules modifies the electrostatic environment around the Menshutkin species and induces a global electric field pointing in the opposite direction of the applied EEF. The combination of these two entangled effects leads to partial or complete screening of the EEF, with the extent of screening being proportional to the polarity/polarizability of the solvent. *Nevertheless, we find that catalysis of the Menshutkin reaction inevitably emerges once the EEF exceeds the opposing field of the organizing solvent, i.e., once polarization of the Menshutkin complex is observed to set in.* Overall, our analysis provides a lucid and pictorial interpretation of the behavior of solutions in the presence of EEFs and indicates that EEF-mediated catalysis should, in principle, be feasible in bulk setups, especially for nonpolar and mildly polar solvents. By application of the charge-transfer paradigm, it is shown that the emergence of OEEF catalysis in solution can be generalized to other reactions as well.

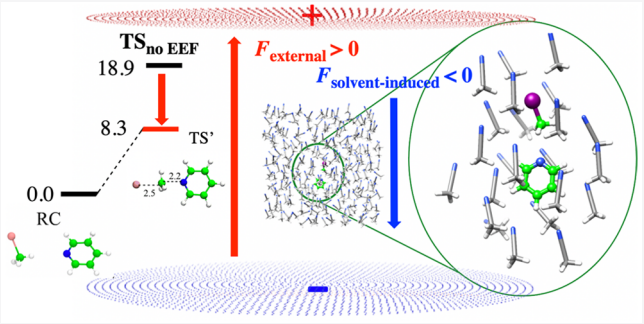

INTRODUCTION

It is well established that external electric fields (EEFs) can affect chemical reactivity and structure.[1,2] By use of a single-molecule scanning tunneling microscopy (STM) experimental setup, Aragonés et al. offered an initial proof of principle that a Diels−Alder reactions, which involves concerted two C−C bond-making, can be catalyzed by EEFs.[3] Since then, multiple groups have used similar setups to probe EEF-mediated reactivity.[4,5] Very recently, Venkataraman and co-workers demonstrated that the *cis/trans* isomerization of cumulenes can be catalyzed and directed in an STM experiment.[6] Other experimental approaches exist which may, in principle, harness electrostatics in chemical reactivity in bulk, involving surface charging,[7] or the generation of interfacial electric fields in non-Faradaic electrochemical cells.[8]

Alternatively, the use of so-called local electric fields (LEFs) has been explored.[1b,c] LEFs are electric fields generated by charged functional groups or dipoles at distant sites of a reactant or catalyst, which can potentially influence the reactivity exhibited at the active site/reactive center.[9−12]

Electric-field-mediated catalysis would become practically useful upon development of scalable and cost-effective methods. Most of the techniques and approaches mentioned above are either not inherently scalable or they put limitations on the structural diversity of the reactants involved in the chemical system under consideration. Some reports on esterification reactions in solvents have recently suggested that pulsed electric fields (PEFs) could impart electrostatic catalysis in a continuous-flow reactor setup.[13] While such an approach would, in principle, be scalable, its broad-range effectiveness has not been demonstrated yet. Importantly, a clear understanding of the effect of the presence of (bulk) solvent on the catalysis effected by EEFs is not yet available, so that the exact mechanism whereby PEFs—or more generally speaking, any EEF in solution—could affect chemical reactivity is currently still clouded.

Received: December 3, 2019
Published: May 5, 2020

https://dx.doi.org/10.1021/jacs.9b13029
J. Am. Chem. Soc. 2020, 142, 9955−9965

The common understanding is that solvent molecules collectively screen any exerted EEF,[1,6] so that in a bulk situation, the global field effect should become—either partially or completely—canceled out. The ability for a solvent to screen an external field is understood to depend on the dielectric constant and polarizability of the solvent, i.e., on its polarity.[14] Additionally, it is known that intense EEFs may cause solvents to evaporate and bring about the breakdown of the solvent molecules or reactants, thus generating currents and many byproducts.[8] These phenomena are often lumped together and are collectively described as "dielectric breakdown".[15] Despite these apparent limitations, there have been several experimental treatments of reactions in solvents under the influence of an EEF by Kanan,[8] Matile,[7] and Ciampi and Coote,[16] and even the STM experiments we have referred to above are carried out in (nonpolar) solvents.[3−5] In the STM study by Venkataraman et al., the influence of different solvents on the catalytic activity exerted by an applied EEF was compared directly, and a significant decrease of catalysis for polar solvents compared to nonpolar ones was found.[6] Furthermore, Cassone et al. used state-of-the-art Car−Parrinello molecular dynamics/density functional theory (CPMD/DFT)[17] calculations to simulate various reactions in water and in alcohol under the influence of an external field and reported a variety of interesting results.[18]

The present paper is focused on shedding some more light on the effect of the presence of solvent on EEF-mediated catalysis. To this end, we have decided to investigate a synthetically useful reaction, the Menshutkin reaction.[19] The reaction system, pyridine and methyl iodide, as well as the convention used for the electric field direction, are shown in Figure 1.

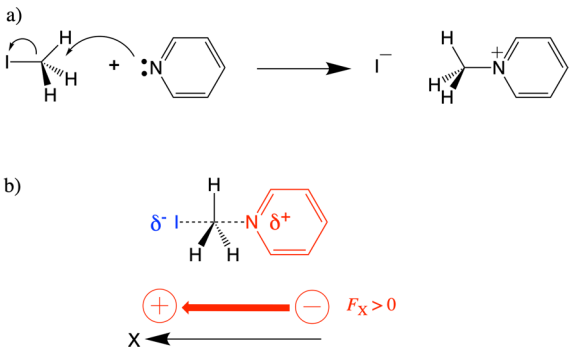

Figure 1. (a) Schematic representation of the Menshutkin reaction of pyridine with methyl iodide. (b) The associated transition-state (TS) geometry, wherein the reaction axis is indicated as a dashed line, and the convention for *a positively oriented* EEF vector along the reaction axis (F_X), which induces catalysis in the gas phase. Note that throughout this work, we employ the Gaussian convention for the electric field direction, i.e., directed from negative to positive.

It has been understood for quite some time that exposing the reaction complex associated with the Menshutkin reaction in the gas phase to an oriented external electric field with $F_X > 0$ along the reaction axis (cf. Figure 1b) induces catalysis, whereas flipping the direction of the field induces inhibition.[1,20] The detailed mechanism behind the catalytic activity of EEFs for this type of gas-phase reactivity has been discussed at length on many different occasions, cf. refs 1a and 1c for a detailed valence bond (VB) treatment, for example. In short, one could say that the EEF induces polarization of the reacting species in the direction which facilitates the "flow" of the electrons throughout the transformation from reactant to the two ionic products, and thereby lowers the reaction barrier and increases the thermodynamic driving force by stabilizing the transition state (TS) and the products. How will the presence of solvent molecules affect this catalysis? That is the question we try to address below.

Throughout our discussions, we will mainly focus on our findings for the prototypical polar solvent CH_3CN (ε = 36.6), but similar trends are observed for the other solvents considered, i.e., chloroform (ε = 4.8) and acetone (ε = 21.0), *vide infra*.[21]

The reaction depicted in Figure 1a will be studied through a combination of molecular dynamics (MD) simulations under the influence of an EEF (F_X, Figure 1) of a varying field strength, followed by quantum mechanical (QM)/molecular mechanical (MM)[22] and quantum mechanical (QM)/electric field (EF)[23,24] calculations. The conceptual picture emerging from these calculations provides a lucid interpretation and pictorial understanding of the ubiquitous solvent screening effect and the behavior of polar solutions in the presence of external electric fields.

METHODOLOGY

Molecular Dynamics of the Solvated Systems. All MD simulations with and without an EEF were carried out using the AMBER18 package.[25] Detailed information about the construction of the solvent boxes for the different solvents, introduction of the Menshutkin complex, and the setup of the MD simulations up to the equilibration step can be found in Section S1 in the Supporting Information (SI). To simulate the effect of electric fields on the full solvated system, an EEF (F_X) was applied in the direction of the reaction coordinate, i.e., in the direction of the N---C---I reaction axis, which is aligned to the $+X$ direction in the modeled system, at different field strengths. We applied F_X values of 0.02, 0.03, 0.035, 0.04, 0.05, 0.06, 0.07, 0.1, 0.15, and 0.2 V/Å using the option "external electric" implemented in the Amber MD package. At each F_X value, we reran the MD simulation. All these production dynamics were each carried out for 10 ns. Since the final few nanoseconds of the simulations revealed no conformational changes in the solvent, the chosen simulation time frame was considered adequate/sufficient. Entropies of all simulated complexes were calculated using the Cpptraj module of the Amber MD package, which makes use of the quasi harmonic approximation method. Let us note that, while our simulations do not include solvent polarization, still this polarization will definitely occur in the solvent molecules, based on the extensive calculations of this effect in molecules subjected to EEFs.[1,2]

Calculation of the Gas-Phase Reaction Profile. The gas-phase PES associated with the Menshutkin reaction was determined by use of Gaussian09.[26] For geometry optimization and frequency calculations, we used the hybrid B3LYP[27] functional and a basis set B1, consisting of Def2-SVP for all atoms. The energies were further corrected with the large all-electron basis set Def2-TZVP, labeled as B2. The zero-point energy (ZPE) was calculated for all species, and all the final energies are reported as UB3LYP/B2+ZPE. Entropic contributions were not taken into account in the constructed potential energy surface; as discussed in Section S3 in the SI, the effect of the entropy on the EEF-mediated catalysis (*vide infra*) can be expected to be minor.

Electrostatic Effect of the Solvent Environment on the Reaction. Two distinct calculations were performed on a representative snapshot of the MD simulation in the absence of an electric field, to determine the effect of the solvent environment on the Menshutkin reaction and assess the extent to which this effect is electrostatic in nature. This representative snapshot was chosen from the clustering of the MD trajectories, which provides the most populated trajectories along with the representative snapshot for each

https://dx.doi.org/10.1021/jacs.9b13029
J. Am. Chem. Soc. 2020, 142, 9955−9965

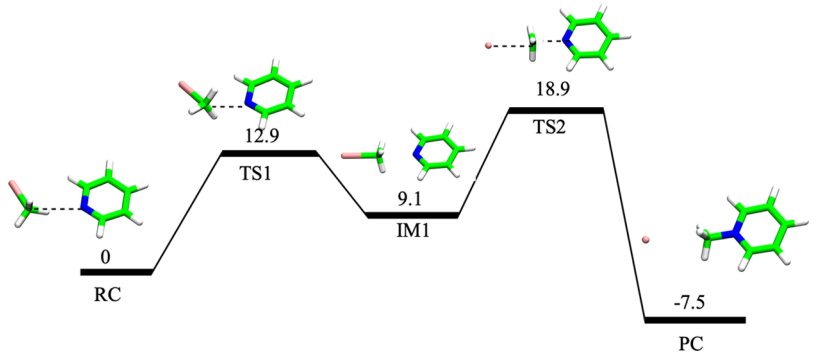

Figure 2. Potential energy surface (PES) associated with the Menshutkin reaction between pyridine and CH_3I in a field-free CH_3CN solvent environment, with its characteristic species indicated as follows: reactant complex (RC), first transition state (TS1), intermediate (IM1), second transition state (TS2), and product complex (PC). Energies (relative to RC) are shown in kcal/mol.

cluster. This protocol is statistically more accurate relative to the stochastically chosen snapshot.[28]

First, a QM/MM calculation was executed such that the reactants, pyridine and methyl iodide, were treated at a QM level of theory, while all solvent molecules were kept as "active MM atoms". This QM/MM calculation was performed using ChemShell,[29,30] combining Turbomole[31] for the QM part and DL_POLY[32] for the MM part using the Amber force field. The electronic embedding scheme was used to account for the polarizing effect of the solvent environment on the QM region. During the geometry optimizations, the QM region was treated by the hybrid B3LYP functional with two basis sets, in accordance with the gas-phase calculations described above. As such, we used basis set B1 for geometry optimization and frequency calculations and corrected the resulting energies with the B2 basis set. The ZPE was again calculated for all species, and all the final energies are reported as UB3LYP/B2+ZPE.

Subsequently, the point-charge distribution associated with the solvent molecules was extracted and inserted into Gaussian 09,[26] to carry out a single-point QM/EF calculation, where EF represents the point charge distribution of the solvent molecules. UB3LYP/B2+ZPE was used here, in order to test the consistency of QM/EF with the QM/MM calculation. Comparison of the reaction barriers emerging from these two calculations then enabled the confirmation of the electrostatic nature of the solvent effects (*vide infra*).

Screening Effect of the Ordered Solvent Environment. To assess the magnitude of the induced-electric field exerted by the ordered solvent on the reaction axis of the reaction complex, the induced field was quantified using the in-house developed TITAN code.[24] First, the ordered solvent environment, extracted from the MD simulation at 0.2 V/Å, was translated into a charge distribution, in which the individual atoms were assigned by TITAN the same charge parameters as in the MD simulations. Subsequently, the oriented electric field exerted along the N---C---I axis was quantified through a calculation of the individual field vectors associated with each of the point charges in this distribution at different positions along this axis according to Coulomb's law.[24]

Effect of an Applied EEF on the Menshutkin Reaction in Solvent Environments. We performed QM/MM calculation of the solvated Menshutkin reaction system under the influence of an EEF exerted along the *X*-axis, in order to assess the effect of the oriented EEF on the potential energy surface (PES) associated with the reaction. A representative snapshot obtained from the MD simulation at 0.2 V/Å was selected as the input geometry for the simulation box. Since DL-POLY does not contain a keyword to take into account the presence of an EEF in QM/MM calculations, a pair of charged circular plates[33] was generated to mimic such a field with the help of the TITAN code.[24] The generated plates consisted of 33 circular rings of charged dummy atoms, with the spacing between each consecutive ring set to 2.8 Å. Both plates were placed 50 Å away from the C-atom in the middle of the N---C---I axis of the reaction complex on the N- and I-ends. The individual charges were set so as to generate a uniform field strength of 0.5 V/Å inside the solvated system.

Subsequently, we subdivided the solvent box into two parts: all solvent molecules within 6 Å around the reaction complex were taken as the "active" MM region. The outer layer of ordered solvent was designated as "inactive" during the QM/MM calculation; hence, its positions remained frozen (cf. Section S2 in the SI). The reproducibility of the so-calculated energy barriers was tested by rotating the plates by 90° and redoing the QM/MM calculations (see Section S10 in the SI).

Note that since all solvent molecules are treated at the MM level of theory in this final QM/MM calculation, the charges on the respective atoms and the bond lengths remain at their fixed parametrized values throughout the entire simulation. This, in turn, does not account for the gradual polarization of the solvent molecules under the influence of an applied EEF and the consequent increase of the counteracting, global induced solvent field, which is expected to attenuate the catalytic effect of the applied EEF (*vide infra*). Similarly, the inability to describe the polarization taking place in the solvent also implies we are unable to calculate "dielectric breakdown" in our present simulations as the electric field strength is increased.

RESULTS AND DISCUSSIONS

Menshutkin Reaction in Solution without EEF. Since the goal of this contribution is to study the effect of EEFs on the reactivity of a solvated reaction complex, we started with an MD simulation devoid of any applied EEF, for the reactants (pyridine + methyl iodide) in a solvent box consisting of CH_3CN molecules. MD simulation leads to the expected conclusion that the solvent network within the box takes on a disordered geometry over the course of the simulation time and is in a constant flux: the overall dipole moment of the simulation box exhibits a great deal of random fluctuation (see Section S4 in the SI). In order to quantify the degree of disorder more directly, we determined the overall entropy of the system, which amounted to 10.0 kcal/(mol·K).

Our QM/MM calculations reveal that even though the solvent molecules are not spatially ordered at any point throughout the MD simulation, still their collective effect on the Menshutkin reaction is significant. Whereas in the gas phase the reaction mechanism associated with this reaction is essentially concerted and exhibits an excessively high barrier of 27.4 kcal/mol (cf. Section S5 in the SI), in the presence of a solvent environment the reaction turns effectively into a stepwise process. Thus, as shown in Figure 2, the initial step in the mechanism involves the formation of a reactive cluster IM1 along the N---C---I axis. The second step involves the actual displacement reaction step.

The effective kinetic barrier for the full process amounts to 18.9 kcal/mol (cf. Section S6 in the SI).[34] Hence, the field-free

https://dx.doi.org/10.1021/jacs.9b13029
J. Am. Chem. Soc. 2020, 142, 9955−9965

solvent environment unequivocally exerts a catalyzing effect.[35] For acetone and chloroform, a similar, though less pronounced, catalysis is observed (cf. Section S7 in the SI). To assess whether this catalysis imparted by the solvent environment is mainly electrostatic in nature, a QM/EF calculation was performed next to the QM/MM calculation (cf. Methodology). In a QM/EF calculation, a regular QM calculation is performed, with the charge distribution associated with the environment taken into account by use of point charges of the solvent molecules. Performing such a calculation for the optimized QM/MM geometries for the critical species associated with the Menshutkin reaction leads to values that deviate 0.5−1.3 kcal/mol from the original QM/MM barriers listed in Figure 2 (cf. Table 1).

Table 1. Energies of the Critical Species for the Menshutkin Reaction in Acetonitrile, Calculated at QM/MM and QM/EF Level of Theory (UB3LYP/B2+ZPE)[a]

Species	QM/MM energy (kcal/mol)	QM/EF energy (kcal/mol)
RC	0.0	0.0
TS1	12.9	13.7
IM	9.1	10.27
TS2	18.9	19.4
PC	−7.5	−6.2

[a]The energy of the respective reactant complex was taken as the reference.

This finding confirms that the effect of the solvent on the main features of the reaction is indeed almost exclusively electrostatic in nature; put differently, this indicates that *the solvent environment can be modeled quite accurately by use of a simple point-charge distribution.*

Using the TITAN code, we were able to quantify the net intrinsic electric field exerted by the solvent molecules, inside the Menshutkin cavity, in the EEF-free reaction. We observe that this field changes dramatically throughout the cavity as the reaction proceeds, due to the dynamic reorganization of the surrounding disordered solvent network (Figure 3).

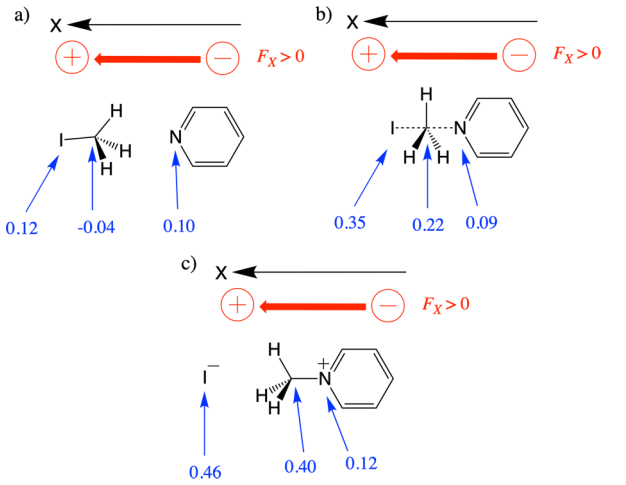

Figure 3. Component of the intrinsic electric field (in V/Å units) aligned with the reaction axis (F_X) at a number of positions throughout the Menshutkin cavity in CH_3CN solvent for (a) the reactant geometry, (b) the TS2 geometry, and (c) the product geometry.

In the reactant geometry, the magnitude of the EF component aligned with the reaction axis fluctuates significantly and takes on both positive and negative values, ranging from −0.04 up to +0.12 V/Å. In the TS2 geometry, on the other hand, the electric field corresponds to a more or less uniform oriented field: F_X is consistently positive across the cavity and remains almost constant in magnitude. In the product geometry, the field strength of this emerging oriented intrinsic electric field increases even further. Note that the orientation of the observed oriented intrinsic electric field matches exactly the field direction needed for catalysis of the Menshutkin reaction (cf. Figure 1). As such, *the solvent itself effectively takes on the role of a catalyzing oriented EF throughout the reaction.*

Note that the appearance of a solvent-induced oriented electric field throughout the reaction is a logical consequence of the gradual polarization occurring within the Menshutkin complex, i.e., the emergence of a positive charge on the pyridine and a negative charge on the iodide moieties. In the proximity of the pyridine, the $CN^{\delta-}$ moieties of the solvent molecules become increasingly directed toward the cavity; in the region around the iodine on the other hand, it is the $CH_3^{\delta+}$ moieties of the molecules, which are increasingly directed toward the Menshutkin complex.

Note also that the differential electrostatic stabilization of the species along the PES by the electrostatic environment of the solvent described above is in fact the basis of the implicit solvent models ubiquitously used in quantum chemistry.[36]

MD Simulations of the Solution under the Influence of an EEF. To assess the effect of EEF application on the reagents and their solvent environment, MD simulations were subsequently performed in the presence of an electric field of incremental strength. For the acetonitrile solvent, the field strength was varied from 0.02 to 0.2 V/Å (0.02, 0.03, 0.035, 0.04, 0.05, 0.06, 0.07, 0.1, 0.15, and 0.2 V/Å). Figure 4 shows the EEF effect on the solvent ordering, where Figure 4a indicates the convention of the polarity of the applied EEF. The solvent distribution around the reactant complex (pyridine + methyl iodide) undergoes a steady evolution from a disordered state, in the absence of an EEF, to an ordered/aligned one as the electric field strength increases. Figure 4b shows the disordered solvent, whereas Figure 4c displays the ordered solvent.

Figure 5 allows a visual inspection of the representative snapshots in the MD trajectories for different F_X values. It is seen that the solvent alignment increases with an increasing strength of F_X, and the global dipole moments of the solvent molecules (red arrows in Figure 5) gradually aligns with the field along the X axis. At $F_X \geq 0.15$ V/Å, almost all CH_3CN molecules are aligned, and so is the global dipole moment. Note that this finding, i.e., that external electric fields induce reorientation and ordering in a liquid phase, is in agreement with previous experimental results[37] and computational results by Evans[38] and Cassone et al.[18,39] as well as by others.[40]

To further elaborate on the effect of EEFs on the solvent ensemble, we also calculated the evolution of the entropy of the solvent as well as the net dipole moment of the system as the EEF strength increases (Figure 6a and b, respectively). It is quite clear that the order as well as the global dipole moment of the ensemble increases gradually with increasing strength of the applied EEF. It is, however, important to note that this initial rise is followed by a leveling off for both the solvent's entropy and dipole moment. As such, there seems to be a

https://dx.doi.org/10.1021/jacs.9b13029
J. Am. Chem. Soc. 2020, 142, 9955−9965

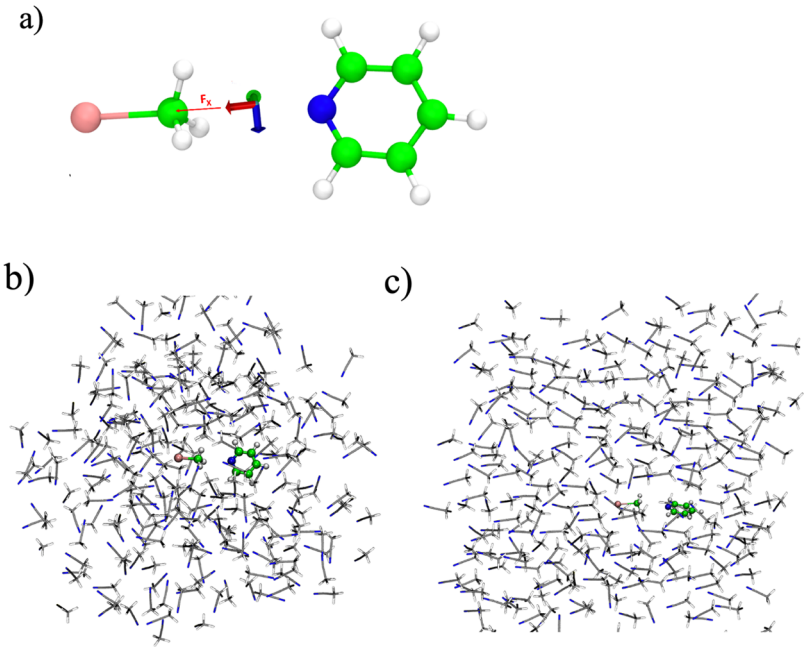

Figure 4. (a) Reaction system and the convention for a positive EEF applied in the study. (b) Disordered polar solvent (CH_3CN), which is obtained when the electric field strength is either zero or very small. (c) Significantly more ordered CH_3CN, which is obtained for a moderately strong electric field, i.e., F_X > 0.1 V/Å. In both parts (b) and (c), the reactants (pyridine---methyl iodide) are present in the middle of the simulation box.

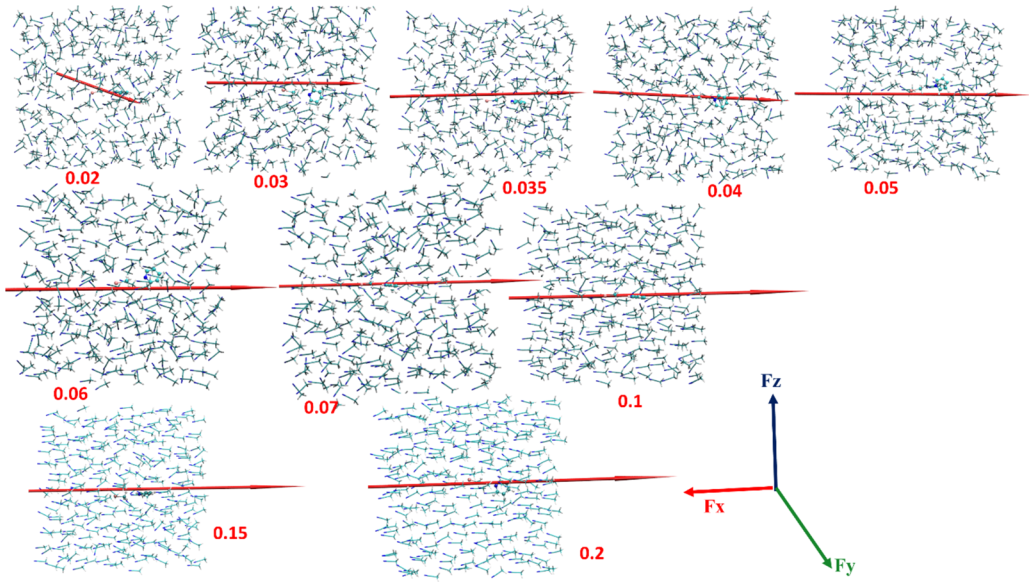

Figure 5. Representative snapshots from MD simulations of a CH_3CN solvent box at different positive F_X values (in V/Å), which are noted in red below (or next to) each individual snapshot. The convention for a positive field is the same as shown in Figure 1a. The red arrows drawn in each frame show the direction of the global dipole moment of the solvent ensemble in the box (in Debye units); the convention for the dipole moment vector assigns the head of the arrow as the positive pole.

critical field strength above which the solution is no longer able to change its structure in response to further increase of the EEF. This observation can be straightforwardly rationalized by realizing that the mechanism through which the solvent responds to the application of an EEF is a collective orientation of the solvent molecules: *at some point the solution will have become perfectly aligned/organized so that the dipole moment can no longer be increased this way; i.e., dielectric saturation of the solution has been reached.*[41]

Further evidence for this reasoning can be found in the observation that for smaller field strengths, e.g., 0.02 V/Å, the standard deviation in dipole moment is ±50 D (Debye), while for stronger EEFs, the standard deviation drops to ±10 D (see the root-mean-square atomic fluctuations in Section S8 in the SI and the evolution of the overall dipole moment of the simulation box in Section S9 in the SI); i.e., at some point a maximal alignment of the individual dipoles is reached. In other words, *one can say that the EEF acts as a tweezer, which*

https://dx.doi.org/10.1021/jacs.9b13029
J. Am. Chem. Soc. 2020, 142, 9955−9965

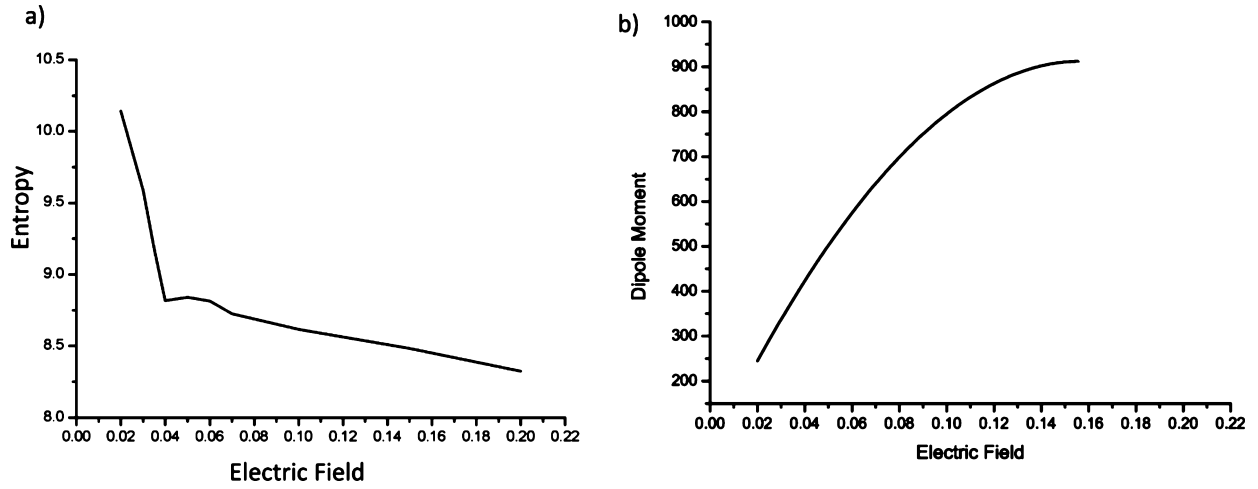

Figure 6. Smoothed plots of (a) the solvent entropy (in kcal/(mol·K)) vs F_X (in V/Å) and (b) the dipole moment (in Debye units) of the CH_3CN solvent system vs F_X (in V/Å).

both aligns the solvent molecules (see also Figures 2c and 6) *and keeps them from fluctuating due to thermal motion.*[42]

For the other solvents tested, i.e., acetone and chloroform, similar qualitative trends are observed, but the calculated critical electric field strength at which perfect solvent alignment, i.e., dielectric saturation, is reached, is shifted upward as the polarity of the solvent decreases (already for acetone, $F_{X,\text{critical}} > 1$ V/Å). This behavior can be connected to the lower individual dipole moments of the $CHCl_3$ and CH_3COCH_3 molecules: *a higher external field strength is needed to overcome thermal fluctuations and produce sufficient stabilization of the perfectly aligned orientation.* This is also reflected in the observation that the growth of the global dipole moment as a function of increasing field strength is reduced for these solvents (cf. Section S9 of the SI).

Note that the use of a non-polarizable force field in our MD overestimates the calculated critical field strength value; in reality, the dipole moment of the individual solvent molecules will increase as the EEF strength grows,[1b] which will facilitate the orientation of the molecules.

How Does the Solvent Ordering Affect the Observed Catalysis? One can logically expect that the emergence of solvent ordering under the influence of an external electric field will significantly impact the solvent-induced catalysis. Recall that the solvent-induced catalysis is essentially a local and dynamic process: the solvent molecules adjacent to the cavity reorganize as the reaction proceeds so that the reacting complex is optimally stabilized at each step throughout the transformation from reactant to product. For the Menshutkin reaction, this essentially means that the solvent environment effectively gives rise to a catalyzing oriented EF of gradually increasing field strength (Figure 3). *Fixing the orientation of the individual molecules by the EEF will obviously hamper the ability of the solvent to produce such a catalyzing oriented field.*

Additionally, the collective ordering of the many layers of dipoles making up the liquid phase induces a global static electric field in its own right (Figure 6). As can be seen from the sketch in Figure 7, *the direction of the resulting solvent-induced electric field points in the opposite direction of the applied EEF.*

The collective orientation of the solvent molecules will thus result in a partial—or complete—cancellation of the effect of the external field, i.e., *the field is "screened"*. The extent of this

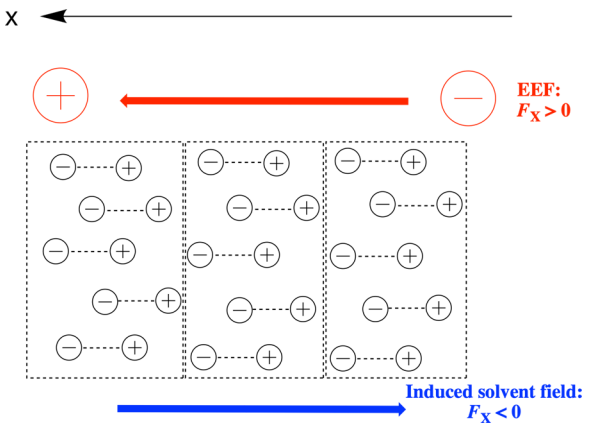

Figure 7. An applied EEF ($F_X > 0$) induces the collective orientation of the dipoles (corresponding to the individual solvent molecules) depicted. The point charge distribution associated with these dipoles in their turn leads to the emergence of an "induced solvent field" ($F_X < 0$), which counteracts the originally applied EEF. Idealized solvent layers are denoted by the dashed boxes. Note the relative displacement of the dipoles within each individual solvent layer, which minimizes the intralayer dipole−dipole repulsion.

screening can be expected to depend mainly on the polarity of the solvent, i.e., the magnitude of the "point charges" on opposite sides of the molecular axis: for strongly polar solvents like acetonitrile, the screening will be almost complete (up to the critical field strength at which perfect orientation is reached, *vide supra*), but for less polar solvents, the organization and screening will be much less pronounced. Another factor which will contribute to the extent of screening is the dimensions of the reaction medium, i.e., the number of layers of solvent molecules which can align collectively.[43]

Our computational results confirm this point of view. We performed QM/MM calculations under the influence of a strong oriented external electric field (OEEF) of 0.5 V/Å for the different solvents (cf. Figure 8 for the geometry of the simulated system in the case of CH_3CN solvent). The EEF was incorporated into the calculation through circular charged capacitor plates, generated with TITAN (cf. Methodology; the plates were included as "inactive atoms" in the MM region). Furthermore, we kept the outer layers of the solvent box frozen in the EEF-aligned orientation obtained from the MD

https://dx.doi.org/10.1021/jacs.9b13029
J. Am. Chem. Soc. 2020, 142, 9955−9965

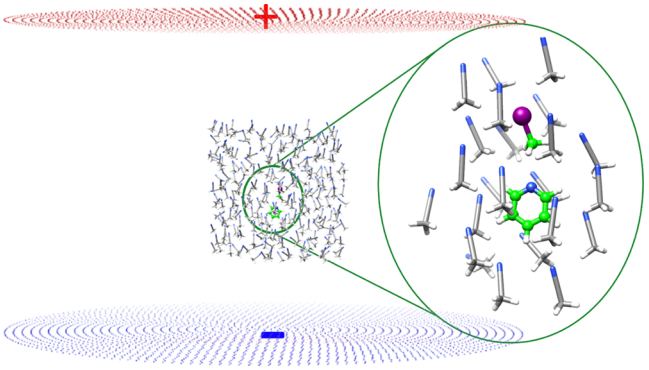

Figure 8. Geometry of the solvated system (in the case of CH_3CN) for the QM/MM calculation under the influence of the EEF. Only the inner MM atoms within 6 Å of reactant were relaxed (i.e., allowed to respond to the EEF), while the rest were kept frozen in the aligned geometry coming out of the MD simulation in the presence of an EEF. Note the solvent orientation around the reaction system in the enlarged view on the right. The red and blue objects are respectively the positively and negatively charged circular plates generated with the help of the TITAN code.

simulation (by making them inactive as well), so as to enforce the shape of the simulation box and thus prevent unphysical separation of the solvent molecules during the simulation (cf. Methodology). The charged plates were placed on opposite sides of the solvent box along the *X*-direction so that the OEEF aligns with the reaction axis of the Menshutkin complex. Note, however, that this choice is in fact trivial since the reaction axis itself (together with all the solvent molecules) will realign itself in the case that the direction of the OEEF is changed, due to the tweezing behavior of the field (cf. Section S10 in the SI).

The calculated PES for the Menshutkin reaction in acetonitrile, in the presence of the OEEF, is shown in Figure 9. Two conclusions can be drawn from this figure: (a) the

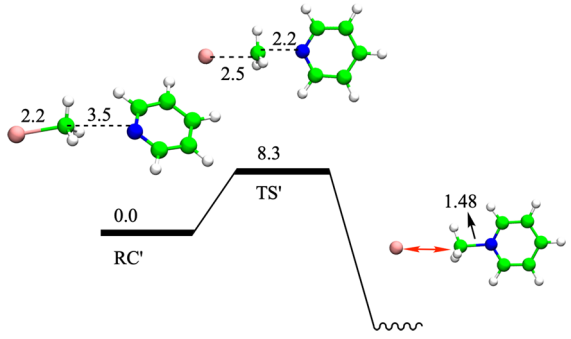

Figure 9. Potential energy surface (PES) associated with the Menshutkin reaction between pyridine and CH_3I in a CH_3CN solvent environment exposed to an EEF of 0.5 V/Å, with its characteristic species indicated: the reactant complex (RC′) and the transition state (TS′). Since no local minimum is observed on the product side of the PES at the considered field strength, the product is represented by a wavy line. Energies are shown in kcal/mol and some key distances are shown in Å.

barrier associated to the first reaction step has completely disappeared now, and (b) the overall barrier for the reaction has dropped significantly.

The disappearance of the barrier for reactive complex formation can be connected to the EEF-induced orientation of the reactants: *the EEF acts as a tweezer that enforces the correct alignment of the reactants, required for the displacement step*, by default. In addition to the OEEF-induced disappearance of the first barrier, one can also observe that the barrier for the overall process has been lowered by the OEEF to 8.3 kcal/mol. Furthermore, no product cluster is formed anymore: once the TS has been crossed, the energy continues to decrease as the charged products separate; i.e., one cannot observe a local minimum on the product side of the PES. Overall, we can unequivocally conclude that the applied field imparts significant catalysis on the solvated system (relative to the barriers of 27.4 and 18.9 kcal/mol in the gas phase and EEF-free solvent, respectively).

For acetone and chloroform, the barriers obtained in the presence of the OEEF are—as expected—lower; they amount to 8.1 and 6.9 kcal/mol, respectively, indicating a somewhat lower extent of screening (cf. Section S11 in the SI).

Analyzing the in-cavity field strength induced by the organized solvent molecules alone, i.e., without taking the charged plates into account, reveals that the enhanced catalysis for chloroform compared to acetonitrile and acetone can indeed be connected to a reduced screening (Figure 10). For

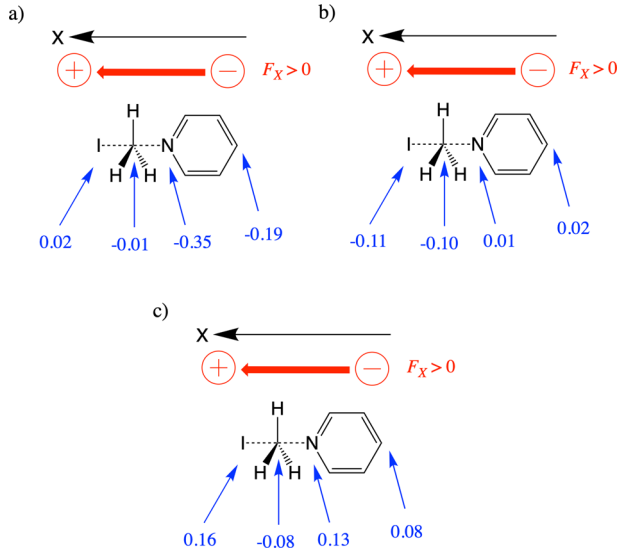

Figure 10. Component of the electric field (in V/Å) aligned with the reaction axis (F_X) exerted by the organized solvent at a number of positions throughout the Menshutkin cavity in the TS geometry for (a) acetonitrile, (b) acetone, and (c) chloroform.

all solvents, the oriented electric field which was present in the field-free solvent situation (cf. Figure 2) has been upended. For chloroform, however, only a very mild (global) counteracting field has emerged, whereas for acetonitrile this counteracting field is significant, and the direction of the original solvent-induced oriented field has essentially been flipped.

Note that solvent polarization in response to the exerted EEF—which was not considered in our QM/MM calculations, cf. Methodology—can generally be expected to increase the strength of the solvent-induced electric field, i.e., enhance the screening. However, once the solvent molecules start to polarize, so will the Menshutkin complex. Since polarization of the reaction complex was exactly what caused EEFs to induce catalysis in the gas-phase situation (cf. Figure 1), catalysis will inevitably emerge as soon as charge separation sets in within the liquid phase, i.e., as soon as the OEEF exceeds the

https://dx.doi.org/10.1021/jacs.9b13029
J. Am. Chem. Soc. 2020, 142, 9955−9965

counteracting field emerging from the collective reorientation of the (unpolarized) solvent molecules.

Finally, we also verified the counteracting nature of the aligned solvent, in its own right, on the Menshutkin reaction. When we extract the geometries of the different critical species coming out of the QM/MM calculation described above and perform a QM/EF calculation on the system, without the OEEF delivered by the charged plates, and with only the point charges associated to the organized solvent taken into account, we find that the energy of the system increases monotonically throughout the entire reaction; i.e., *the solvent-induced electric field, in its own right, indeed inhibits the reaction (and product formation) altogether*.

The slopes of the resulting monotonically increasing energy curves are solvent-polarity-dependent and thus reflective of the magnitude of the generated solvent-induced electric field, in line with what one would expect from the discussion above. Thus, for acetonitrile, we find that the energy of the original TS geometry in the presence of the solvent-induced field amounts to 21.6 kcal/mol. For acetone, this value decreases to 19.5 kcal/mol, and for chloroform, the corresponding energy amounts to barely 13.0 kcal/mol.

Finally, let us reconsider whether the experimental data available in the literature also support the expectations outlined above. As indicated already in the Introduction, STM experiments in the presence of nonpolar solvents indeed lead to catalysis in a similar way as one would expect in the gas phase.[3−5] Furthermore, as tested by Venkataraman et al., upon replacing the nonpolar solvents by polar ones, the catalytic activity of the EEF decreases steadily when the field strength is kept constant.[6] Both of these observations are in agreement with what one would expect based on our pictorial analysis.

Generality of the Model of OEEF Effects in a Solvent. Despite the fact that the preceding discussion focused on a single reaction, our model and conclusions are generalizable, since the catalysis exerted by electric fields follows a universal paradigm. As discussed in our previous studies,[1a,b,2a] and briefly mentioned in the Introduction of this paper, electric fields impart catalysis by disproportionally stabilizing the so-called "VB charge transfer states (CTS)", which are responsible for the charge flow from one reactant to the other and thus for the emergence of polarization within the reaction complex.

Generally, these CTS states do not contribute in an equal way to all the species along the PES; some stationary points are more affected by them than others, and it is this differential susceptibility along the PES which causes the catalysis, i.e., the reduction of the global barrier associated to the process.

For the Menshutkin reaction, the CTS contribution (which—as indicated above—is related to the extent of polarization, i.e., the rise in the magnitude of the dipole moment of the species) increases throughout the entire reaction course, so that both the TS and PC are stabilized by the field relative to the RC.

Other reactions can be discussed in a similar manner, since all reactions possess CTSs. For example, in the Diels−Alder reaction of cyclopentadiene and maleic anhydride,[1,2a] and in oxidative addition reactions,[2b] e.g., the reaction between $P(PH_3)_2$ and CH_3X, it is mainly the TS which is disproportionately stabilized by the field. In any case, since the energy difference between RC and TS decreases for all these reactions, the kinetics will improve under the influence of an electric field, i.e., catalysis sets in.

From our current analysis, one can conclude that the OEEF enhancement of the CTS effect transpires easily in the presence of apolar or mildly polar solvents, where solvent organization by the field will not be so significant (e.g., see $CHCl_3$ and to a lesser extent acetone), but may also take place in strongly polar solvents such as CH_3CN, as soon as the OEEF overcomes the screening.

Whether or not the reactants are pre-organized (or not oriented in the right way for reaction to occur) will play only a minor role in the catalysis: polar reactants will generally become oriented in the correct direction for reaction to occur; i.e., the negative pole of one reagent will be directed toward the positive pole of the other in the field direction (cf. the Menshutkin complex in Figure 1). For apolar reactants, the EEF-mediated pre-organization may not always be favorable, but due to the small dipole moment of these compounds at the onset of the reaction, reorientation will be facile. As such, the energy lowering of the TS, caused by the improved mixing of the CTSs as the reaction proceeds, will still dominate the shape of the PES, and catalysis will emerge.

CONCLUSIONS

To summarize, let us consider the overall picture that emerges from our analysis. Our calculations indicate that, in the absence of an EEF, solvents take on a catalyzing function by gradually developing an oriented intrinsic electric field, facilitating the "electron flow" associated with the transformation from reactants to products. Applying an OEEF causes the solvent to undergo organization; i.e., the solvent molecules gradually align with the applied field as the field strength increases. This collective organization has a major impact on the catalysis provided by the solvent. On one hand, it restricts the positioning of the solvent molecules around the reagent cavity, thus subduing the emergence of the (local) solvent-induced uniform oriented field. On the other hand, it induces a global electric field pointing in the opposite direction of the applied EEF. The combination of these two intertwined effects leads to (partial or complete) screening of the OEEF, with the extent of screening being proportional to the polarity/polarizability of the solvent.

Nevertheless, even though the applied OEEF is clearly attenuated by the solvent environment, *we observe for each of the solvents tested that catalysis inevitably emerges once the OEEF exceeds the opposing field of the organizing solvent and polarization of the Menshutkin complex sets in*. Overall, our analysis provides a lucid and pictorial interpretation of the behavior of solutions in the presence of OEEFs and indicates that OEEF-mediated catalysis should, in principle, be feasible in bulk setups, especially for nonpolar and mildly polar solvents. As shown above, these conclusions and the eventual emergence of catalysis are not particular to the Menshutkin reaction but can be generalized to other reactions as well.

ASSOCIATED CONTENT

Supporting Information

The Supporting Information is available free of charge at https://pubs.acs.org/doi/10.1021/jacs.9b13029.

Detailed information concerning the molecular dynamics simulations, technical motivation for the subdivision of the solvent box, estimation of the entropic contribution to the observed catalysis, evolution of the overall dipole moment of the simulation box over time

https://dx.doi.org/10.1021/jacs.9b13029
J. Am. Chem. Soc. 2020, 142, 9955−9965

(F_X = 0), gas-phase reaction profile of the Menshutkin reaction, effective kinetic barrier for the full Menshutkin reaction in acetonitrile depicted in Figure 2 of the main text, potential energy surface associated with the Menshutkin reaction between pyridine and CH_3I in a field-free acetone and chloroform solvent, root-mean-square deviation of the solvent at three different EEF field strengths, evolution of the overall dipole moment of the simulation box over time ($F_X \neq 0$), realignment of the solvent and reaction axes upon application of an OEEF aligned with the y-axis, simulation results for acetone and chloroform ($F_X \neq 0$), and geometries for all the QM systems (PDF)

AUTHOR INFORMATION

Corresponding Authors

Kshatresh Dutta Dubey − *Department of Chemistry & Center for Informatics, Shiv Nadar University, Greater Noida, Uttar Pradesh 201314, India;* orcid.org/0000-0001-8865-7602; Email: kshatresh@gmail.com

Thijs Stuyver − *Institute of Chemistry, Edmond J. Safra Campus at Givat Ram, The Hebrew University, Jerusalem 9190400, Israel; Algemene Chemie, Vrije Universiteit Brussel, 1050 Brussels, Belgium;* orcid.org/0000-0002-8322-0572; Email: thijs.stuyver@mail.huji.ac.il

Sason Shaik − *Institute of Chemistry, Edmond J. Safra Campus at Givat Ram, The Hebrew University, Jerusalem 9190400, Israel;* orcid.org/0000-0001-7643-9421; Email: sason.shaik@gmail.com

Author

Surajit Kalita − *Department of Chemistry & Center for Informatics, Shiv Nadar University, Greater Noida, Uttar Pradesh 201314, India*

Complete contact information is available at: https://pubs.acs.org/10.1021/jacs.9b13029

Author Contributions

‖K.D.D. and T.S. contributed equally.

Notes

The authors declare no competing financial interest.

ACKNOWLEDGMENTS

K.D.D. acknowledges the Department of Biotechnology, Govt of India for a Ramalingamswami re-entry research grant (BT/RLS/Re-entry/10/2017). T.S. acknowledges the Research Foundation-Flanders (FWO) for a position as postdoctoral research fellow (1203419N). S.S. is supported by the Israel Science Foundation (ISF 520/18).

REFERENCES

(1) (a) Shaik, S.; Mandal, D.; Ramanan, R. Oriented Electric Fields as Future Smart Reagents in Chemisty. *Nat. Chem.* **2016**, *8*, 1091−1098. (b) Shaik, S.; Ramanan, R.; Danovich, D.; Mandal, D. Structure and reactivity/selectivity control by oriented-external electric fields. *Chem. Soc. Rev.* **2018**, *47*, 5125−5145. (c) Ciampi, S.; Darwish, N.; Aitken, H. M.; Diez-Pérez, I.; Coote, M. L. Harnessing electrostatic catalysis in single molecule, electrochemical and chemical systems: a rapidly growing experimental tool box. *Chem. Soc. Rev.* **2018**, *47*, 5146−5164. (d) Stuyver, T.; Danovich, D.; Joy, J.; Shaik, S. External electric field effects on chemical structure and reactivity. *Wiley Interdiscip. Rev.: Comput. Mol. Sci.* **2020**, *10*, e1438. (e) Wang, Z.; Danovich, D.; Ramanan, R.; Shaik, S. Oriented-external electric fields create absolute enantioselectivity in Diels-Alder reactions: The importance of the molecular dipole moment. *J. Am. Chem. Soc.* **2018**, *140*, 13350−13359.

(2) (a) Meir, R.; Chen, H.; Lai, W.; Shaik, S. Oriented Electric Fields Accelerate Diels-Alder Reactions and Control the endo/exo Selectivity. *ChemPhysChem* **2010**, *11*, 301−310. (b) Joy, J.; Stuyver, T.; Shaik, S. External electric fields and ionic additives elicit catalysis and mechanistic crossover in oxidative addition reactions. *J. Am. Chem. Soc.* **2020**, *142*, 3836−3850. (c) Yu, L.-J.; Coote, M. L. Electrostatic Switching between SN1 and SN2 Pathways. *J. Phys. Chem. A* **2019**, *123*, 582−589. (d) Harzmann, G. D.; Frisenda, R.; van der Zant, H. S. J.; Mayor, M. Single-Molecule Spin Switch Based on Voltage- Triggered Distortion of the Coordination Sphere. *Angew. Chem., Int. Ed.* **2015**, *54*, 13425−13430. (e) Velpula, G.; Teyssandier, J.; De Feyter, S.; Mali, K. S. Nanoscale Control over the Mixing Behavior of Surface-Confined Bicomponent Supramolecular Networks Using an Oriented External Electric Field. *ACS Nano* **2017**, *11*, 10903−10913. (f) Oklejas, V.; Uibel, R. H.; Horton, R.; Harris, J. M. Electric-Field Control of the Tautomerization and Metal Ion Binding Reactivity of 8-Hydroxyquinoline Immobilized to an Electrode Surface. *Anal. Chem.* **2008**, *80*, 1891−1901. (g) Rincón, L.; Mora, J. R.; Torres, F. J.; Almeida, R. On the Activation of σ-bonds by electric fields: A Valence Bond Perspective. *Chem. Phys.* **2016**, *477*, 1−7. (h) Foroutan-Nejad, C.; Andrushchenko, V.; Straka, M. Dipolar Molecules Inside C70: An Electric Field-Driven Room-Temperature Single-Molecule Switch. *Phys. Chem. Chem. Phys.* **2016**, *18*, 32673−32677. (i) Bandrauk, A. D.; Sedik, E-W. S.; Matta, C. F. Effect of Absolute Laser Phase on Reaction Paths in Laser-Induced Chemical Reactions. *J. Chem. Phys.* **2004**, *121*, 7764−7775. (j) Schirmer, B.; Grimme, S. Electric Field Induced Activation of H2-Can DFT do the job? *Chem. Commun.* **2010**, *46*, 7942−7944. (k) Bhattacharyya, K.; Karmakar, S.; Datta, A. External Electric Field Control: Driving the Reactivity of Metal-Free Azide-Alkyne Click Reactions. *Phys. Chem. Chem. Phys.* **2017**, *19*, 22482−22486. (m) Papanikolaou, P.; Karafiloglou, P. Investigating Sigma Bonds in An Electric Field from the Paulings Perspective: The Behavior of Cl-X and H-X (X = C,Si) Bonds. *Theor. Chem. Acc.* **2010**, *126*, 213−222. (n) Karafiloglou, P. Control of Delocalization and Structural Changes by Means of An Electric Field. *J. Comput. Chem.* **2006**, *27*, 1883−1891. (o) Arabi, A. A.; Matta, C. F. Effects of External Electric Fields on Double Proton Transfer Kinetics in the Formic Acid Dimer. *Phys. Chem. Chem. Phys.* **2011**, *13*, 13738−13748. (p) Saitta, A. M.; Saija, F. Miller Experiments in Atomistic Computer Simulations. *Proc. Natl. Acad. Sci. U. S. A.* **2014**, *111*, 13768−13773. (q) Li, H.; Su, T. A.; Zhang, V.; Steigerwald, M. L.; Nuckolls, C.; Venkataraman, L. Electric Field Breakdown in Single Molecule Junctions. *J. Am. Chem. Soc.* **2015**, *137*, 5028−5033. (r) Darwish, N.; Aragonés, A. C.; Darwish, T.; Ciampi, S.; Díez-Pérez, I. Multi-Responsive Photo- and Chemo-Electrical Single-Molecule Switches. *Nano Lett.* **2014**, *14*, 7064−7070. (s) Jaros, A.; Farajpour Bonab, E.; Straka, M.; Foroutan-Nejad, C. Fullerene-Based Switching Molecular Diodes Controlled by Oriented External Electric Fields. *J. Am. Chem. Soc.* **2019**, *141*, 19644−19654. (l) Stuyver, T.; Ramanan, R.; Mallick, D.; Shaik, S. Oriented (local) electric fields drive the millionfold enhancement of the H-abstraction catalysis observed for synthetic metalloenzyme analogues. *Angew. Chem., Int. Ed.* **2020**, *59*, 7915.

(3) Aragonés, A. C.; Haworth, N. L.; Darwish, N.; Ciampi, S.; Bloomfield, N. J.; Wallace, G. G.; Diez-Perez, I.; Coote, M. L. Electrostatic Catalysis of a Diels-Alder Reaction. *Nature* **2016**, *531*, 88−91.

(4) (a) Borca, B.; Michnowicz, T.; Pétuya, R.; Pristl, M.; Schendel, V.; Pentegov, I.; Kraft, U.; Klauk, H.; Wahl, P.; Gutzler, R.; Arnau, A.; Schlickum, U.; Kern, K. Electric-field-driven direct desulfurization. *ACS Nano* **2017**, *11*, 4703−4709. (b) Zhang, L.; Laborda, E.; Darwish, N.; Noble, B. B.; Tyrell, J. H.; Pluczyk, S.; Le Brun, A. P.; Wallace, G. G.; Gonzalez, J.; Coote, M.; Ciampi, S. Electrochemical and electrostatic cleavage of alkoxyamines. *J. Am. Chem. Soc.* **2018**, *140*, 766−774. (c) Reecht, G.; Lotze, C.; Sysoiev, D.; Huhn, T.; Franke, K. J. Disentangling electron-and electric-field-induced ring-

closing reactions in a diarylethene derivative on Ag (1 1 1). *J. Phys.: Condens. Matter* **2017**, *29*, 294001.
(5) Huang, X.; Tang, C.; Li, J.; Chen, L. C.; Zheng, J.; Zhang, P.; Le, J.; Li, R.; Li, X.; Liu, J.; Yang, Y.; Shi, J.; Chen, Z.; Bai, M.; Zhang, H. L.; Xia, H.; Cheng, J.; Tian, Z. Q.; Hong, W. Electric field−induced selective catalysis of single-molecule reaction. *Sci. Adv.* **2019**, *5*, eaaw3072.
(6) Zang, Y.; Zou, Q.; Fu, T.; Ng, F.; Fowler, B.; Yang, J.; Li, H.; Steigerwald, M. L.; Nuckolls, C.; Venkataraman, L. Directing isomerization reactions of cumulenes with electric fields. *Nat. Commun.* **2019**, *10*, 4482.
(7) Akamatsu, M.; Sakai, N.; Matile, S. Electric-field-assisted anion−π catalysis. *J. Am. Chem. Soc.* **2017**, *139*, 6558−6561.
(8) (a) Gorin, C. F.; Beh, E. S.; Kanan, M. W. An Electric Field−Induced Change in the Selectivity of a Metal Oxide−Catalyzed Epoxide Rearrangement. *J. Am. Chem. Soc.* **2012**, *134*, 186−189. (b) Gorin, C. F.; Beh, E. S.; Bui, Q. M.; Dick, G. R.; Kanan, M. W. Interfacial electric field effects on a carbene reaction catalyzed by Rh porphyrins. *J. Am. Chem. Soc.* **2013**, *135*, 11257−11265.
(9) (a) Pocker, Y.; Buchholz, R. F. Electrostatic catalysis of ionic aggregates. I. Ionization and dissociation of trityl chloride and hydrogen chloride in lithium perchlorate-diethyl ether solutions. *J. Am. Chem. Soc.* **1970**, *92*, 2075−2084. (b) Pocker, Y.; Buchholz, R. F. Electrostatic catalysis by ionic aggregates. II. Reversible elimination of hydrogen chloride from tert-butyl chloride and the rearrangement of 1-phenylallyl chloride in lithium perchlorate-diethyl ether solutions. *J. Am. Chem. Soc.* **1970**, *92*, 4033−4038.
(10) Warshel, A.; Sharma, P. K.; Kato, M.; Xiang, Y.; Liu, H.; Olsson, M. H. Electrostatic basis for enzyme catalysis. *Chem. Rev.* **2006**, *106*, 3210−3235.
(11) (a) Geng, C.; Li, J.; Weiske, T.; Schlangen, M.; Shaik, S.; Schwarz, H. Electrostatic and charge-induced methane activation by a concerted double C−H bond insertion. *J. Am. Chem. Soc.* **2017**, *139*, 1684−1689. (b) Schwarz, H.; Shaik, S.; Li, J. Electronic effects on room-temperature, gas-phase C−H Bond activations by cluster oxides and metal carbides: The methane challenge. *J. Am. Chem. Soc.* **2017**, *139*, 17201−17212.
(12) (a) Klinska, M.; Smith, L. M.; Gryn'ova, G.; Banwell, M. G.; Coote, M. L. Experimental demonstration of pH-dependent electrostatic catalysis of radical reactions. *Chem. Sci.* **2015**, *6*, 5623−5627. (b) Aitken, H. M.; Coote, M. L. Can electrostatic catalysis of Diels−Alder reactions be harnessed with pH-switchable charged functional groups? *Phys. Chem. Chem. Phys.* **2018**, *20*, 10671−10676.
(13) Lin, Z. R.; Zeng, X. A.; Yu, S. J.; Sun, D. W. Enhancement of ethanol−acetic acid esterification under room temperature and non-catalytic condition via pulsed electric field application. *Food Bioprocess Technol.* **2012**, *5*, 2637−2645.
(14) (a) Andzelm, J.; Kölmel, C.; Klamt, A. Incorporation of solvent effects into density functional calculations of molecular energies and geometries. *J. Chem. Phys.* **1995**, *103*, 9312−9320. (b) Eckert, F.; Klamt, A. Fast solvent screening via quantum chemistry: COSMO-RS approach. *AIChE J.* **2002**, *48*, 369−385.
(15) (a) Watson, P. K.; Chadband, W. G.; Sadeghzadeh-Araghi, M. The role of electrostatic and hydrodynamic forces in the negative-point breakdown of liquid dielectrics. *IEEE Trans. Electr. Insul.* **1991**, *26*, 543−559. Jones, H. M.; Kunhardt, E. E. Pulsed dielectric breakdown of pressurized water and salt solutions. *J. Appl. Phys.* **1995**, *77*, 795−805.
(16) Vogel, Y. B.; Zhang, L.; Darwish, N.; Goncales, V. R.; Le Brun, A.; Gooding, J. J.; Molina, A.; Wallace, G. G.; Coote, M. L.; Gonzalez, J.; Ciampi, S. Reproducible flaws unveil electrostatic aspects of semiconductor electrochemistry. *Nat. Commun.* **2017**, *8*, 2066.
(17) Car, R.; Parrinello, M. Unified approach for molecular dynamics and density-functional theory. *Phys. Rev. Lett.* **1985**, *55*, 2471.
(18) (a) Cassone, G.; Sponer, J.; Sponer, J. E.; Pietrucci, F.; Saitta, A. M.; Saija, F. Synthesis of (D)-Erythrose from Glycolaldehyde Aqueous Solutions under Electric Field. *Chem. Commun.* **2018**, *54*, 3211−3214. (b) Cassone, G.; Pietrucci, F.; Saija, F.; Guyot, F.; Sponer, J.; Sponer, J. E.; Saitta, A. M. Novel Electrochemical Route to Cleaner Fuel Dimethyl Ether. *Sci. Rep.* **2017**, *7*, 6901. (c) Cassone, G.; Pietrucci, F.; Saija, F.; Guyot, F.; Saitta, A. M. One-step electric-field driven methane and formaldehyde synthesis from liquid methanol. *Chem. Sci.* **2017**, *8*, 2329−2336. (d) Cassone, G.; Sofia, A.; Rinaldi, G.; Sponer, J. Catalyst-Free Hydrogen Synthesis From Liquid Ethanol: an ab initio Molecular Dynamics Study. *J. Phys. Chem. C* **2019**, *123*, 9202−9208.
(19) (a) Sola, M.; Lledos, A.; Duran, M.; Bertran, J.; Abboud, J. L. M. Analysis of solvent effects on the Menshutkin reaction. *J. Am. Chem. Soc.* **1991**, *113*, 2873−2879. (b) Su, P.; Ying, F.; Wu, W.; Hiberty, P. C.; Shaik, S. The Menshutkin reaction in the gas phase and in aqueous solution: a valence bond study. *ChemPhysChem* **2007**, *8*, 2603−2614.
(20) Ramanan, R.; Danovich, D.; Mandal, D.; Shaik, S. Catalysis of methyl transfer reactions by oriented external electric fields: Are gold−thiolate linkers innocent? *J. Am. Chem. Soc.* **2018**, *140*, 4354−4362.
(21) (a) Weaver, J. H.; Frederikse, H. P. R. *CRC Handbook of Chemistry and Physics*; CRC Press: Boca Raton, FL, 1977. (b) Vogel, A. I. *Practical Organic Chemistry*; Long Man Group Ltd: London, 1974.
(22) Senn, H. M.; Thiel, W. QM/MM methods for biomolecular systems. *Angew. Chem., Int. Ed.* **2009**, *48* (7), 1198−1229.
(23) Schyman, P.; Lai, W.; Chen, H.; Wang, Y.; Shaik, S. The directive of the protein: how does cytochrome P450 select the mechanism of dopamine formation? *J. Am. Chem. Soc.* **2011**, *133*, 7977−7984.
(24) Stuyver, T.; Huang, J.; Mallick, D.; Danovich, D.; Shaik, S. TITAN: A Code for Modeling and Generating Electric Fields—Features and Applications to Enzymatic Reactivity. *J. Comput. Chem.* **2020**, *41*, 74−82.
(25) Case, D. A.; Cheatham, T. E., III; Darden, T.; Gohlke, H.; Luo, R.; Merz, K. M., Jr; Onufriev, A.; Simmerling, C.; Wang, B.; Woods, R. J. The Amber biomolecular simulation programs. *J. Comput. Chem.* **2005**, *26*, 1668−1688.
(26) Frish, M. J.; Trucks, G. W.; Schlegel, H. B.; Scuseria, G. E.; Robb, M. A.; Cheeseman, J. R.; Scalmani, G.; Barone, V.; Mennucci, B.; Petersson, G. A.; Nakatsuji, H.; Caricato, M.; Li, X.; Hratchian, H. P.; Izmaylov, A. F.; Bloino, J.; Zheng, G.; Sonnenberg, J. L.; Hada, M.; Ehara, M.; Toyota, K.; Fukuda, R.; Hasegawa, J.; Ishida, M.; Nakajima, T.; Honda, Y.; Kitao, O.; Nakai, H.; Vreven, T.; Montgomery, J. A., Jr.; Peralta, J. E.; Ogliaro, F.; Bearpark, M.; Heyd, J. J.; Brothers, E.; Kudin, K. N.; Staroverov, V. N.; Keith, T.; Kobayashi, R.; Normand, J.; Raghavachari, K.; Rendell, A.; Burant, J. C.; Iyengar, S. S.; Tomasi, J.; Cossi, M.; Rega, N.; Millam, J. M.; Klene, M.; Knox, J. E.; Cross, J. B.; Bakken, V.; Adamo, C.; Jaramillo, J.; Gomperts, R.; Stratmann, R. E.; Yazyev, O.; Austin, A. J.; Cammi, R.; Pomelli, C.; Ochterski, J. W.; Martin, R. L.; Morokuma, K.; Zakrzewski, V. G.; Voth, G. A.; Salvador, P.; Dannenberg, J. J.; Dapprich, S.; Daniels, A. D.; Farkas, O.; Foresman, J. B.; Ortiz, J. V.; Cioslowski, J.; Fox, D. J. *Gaussian 09*, revision D.01; Gaussian, Inc.: Wallingford, CT, 2013.
(27) (a) Becke, A. D. Density-functional exchange-energy approximation with correct asymptotic behavior. *Phys. Rev. A: At., Mol., Opt. Phys.* **1988**, *38*, 3098−3100. (b) Lee, C.; Yang, W.; Parr, R. G. Development of the Colle-Salvetti correlation-energy formula into a functional of the electron density. *Phys. Rev. B: Condens. Matter Mater. Phys.* **1988**, *37*, 785−789. (c) Stephens, P. J.; Devlin, F. J.; Chabalowski, C.; Frisch, M. J. Ab initio calculation of vibrational absorption and circular dichroism spectra using density functional force fields. *J. Phys. Chem.* **1994**, *98*, 11623−11627. (d) Grimme, S. Semiempirical GGA-type density functional constructed with a long-range dispersion correction. *J. Comput. Chem.* **2006**, *27*, 1787−1799.
(28) Dubey, K. D.; Wang, B.; Vajpai, M.; Shaik, S. MD simulations and QM/MM calculations show that single-site mutations of cytochrome P450 BM3 alter the active site's complexity and the chemoselectivity of oxidation without changing the active species. *Chem. Sci.* **2017**, *8*, 5335−5344.

https://dx.doi.org/10.1021/jacs.9b13029
J. Am. Chem. Soc. 2020, 142, 9955−9965

(29) (a) Metz, S.; Kästner, J.; Sokol, A. A.; Keal, T. W.; Sherwood, P. C hem S hell—a modular software package for QM/MM simulations. *Wiley Interdiscip. Rev.: Comput. Mol. Sci.* **2014**, *4*, 101−110. (b) Sherwood, P.; de Vries, A. H.; Guest, M. F.; Schreckenbach, G.; Catlow, C. R. A.; French, S. A.; Sokol, A. A.; Bromley, S. T.; Thiel, W.; Turner, A. J.; Billeter, S.; Terstegen, F.; Thiel, S.; Kendrick, J.; Rogers, S. C.; Casci, J.; Watson, M.; King, F.; Karlsen, E.; Sjøvoll, M.; Fahmi, A.; Schäfer, A.; Lennartz, C. QUASI: A general purpose implementation of the QM/MM approach and its application to problems in catalysis. *J. Mol. Struct.: THEOCHEM* **2003**, *632*, 1−28.
(30) Kästner, J.; Carr, J. M.; Keal, T. W.; Thiel, W.; Wander, A.; Sherwood, P. DL-FIND: an open-source geometry optimizer for atomistic simulations. *J. Phys. Chem. A* **2009**, *113*, 11856−11865.
(31) Ahlrichs, R.; Bar, M.; Haser, M.; Horn, H.; Kolmel, C. Electronic structure calculations on workstation computers: The program system turbomole. *Chem. Phys. Lett.* **1989**, *162*, 165−169.
(32) Smith, W.; Yong, C. W.; Rodger, P. M. DL_POLY: Application to molecular simulation. *Mol. Simul.* **2002**, *28*, 385−471.
(33) Lai, W.; Chen, H.; Cho, K. B.; Shaik, S. External electric field can control the catalytic cycle of cytochrome P450cam: a QM/MM Study. *J. Phys. Chem. Lett.* **2010**, *1*, 2082−2087.
(34) Kozuch, S.; Shaik, S. How to conceptualize catalytic cycles? The energetic span model. *Acc. Chem. Res.* **2011**, *44*, 101−110.
(35) Su, P.; Ying, F.; Wu, W.; Hiberty, P. C.; Shaik, S. The Menshutkin reaction in the gas phase and in aqueous solution: a valence bond study. *ChemPhysChem* **2007**, *8*, 2603−2614.
(36) Tomasi, J.; Mennucci, B.; Cammi, R. Quantum mechanical continuum solvation models. *Chem. Rev.* **2005**, *105*, 2999−3094.
(37) Evans, M.; Moutran, R.; Price, A. H. Dielectric properties, refractive index and far infrared spectrum of cholesteryl oleyl carbonate. *J. Chem. Soc., Faraday Trans. 2* **1975**, *71*, 1854−1862.
(38) (a) Evans, M. W. Molecular dynamics simulation of induced anisotropy. I. Equilibrium properties. *J. Chem. Phys.* **1982**, *76*, 5473−5479. (b) Evans, M. W. Molecular dynamics simulation of liquid anisotropy. II. Rise and fall transients on a picosecond time scale. *J. Chem. Phys.* **1982**, *76*, 5480−5483. (c) Evans, M. W. Computer simulation of liquid anisotropy. III. Dispersion of the induced birefringence with a strong alternating field. *J. Chem. Phys.* **1982**, *77* (77), 4632−4635. (d) Evans, M. W. Computer simulation of liquid anisotropy. V. Nonlinear molecular dynamics at high field strengths. *J. Chem. Phys.* **1983**, *78*, 925−930. (e) Evans, M. W. Computer simulation of liquid anisotropy. IV. Terms to second order in the external field of force. *J. Chem. Phys.* **1983**, *78*, 5403−5407.
(39) Cassone, G.; Sponer, J.; Trusso, S.; Saija, F. Ab initio spectroscopy of water under electric fields. *Phys. Chem. Chem. Phys.* **2019**, *21*, 21205−21212.
(40) (a) Choi, Y. C.; Pak, C.; Kim, K. S. Electric field effects on water clusters (n= 3−5): Systematic ab initio study of structures, energetics, and transition states. *J. Chem. Phys.* **2006**, *124*, No. 094308. (b) James, T.; Wales, D. J.; Hernández Rojas, J. Energy landscapes for water clusters in a uniform electric field. *J. Chem. Phys.* **2007**, *126*, No. 054506. (c) Shafiei, M.; von Domaros, M.; Bratko, D.; Luzar, A. Anisotropic structure and dynamics of water under static electric fields. *J. Chem. Phys.* **2019**, *150*, No. 074505. (d) Winarto; Yamamoto, E.; Yasuoka, K. Water molecules in a carbon nanotube under an applied electric field at various temperatures and pressures. *Water* **2017**, *9*, 473. (e) Futera, Z.; English, N. J. Communication: Influence of external static and alternating electric fields on water from long-time non-equilibrium ab initio molecular dynamics. *J. Chem. Phys.* **2017**, *147*, No. 031102. (f) Sellner, B.; Valiev, M.; Kathmann, S. M. Charge and electric field fluctuations in aqueous NaCl electrolytes. *J. Phys. Chem. B* **2013**, *117*, 10869−10882. (g) Kathmann, S. M.; Kuo, I. F. W.; Mundy, C. J. Electronic effects on the surface potential at the vapor− liquid interface of water. *J. Am. Chem. Soc.* **2008**, *130*, 16556−16561.
(41) (a) Grahame, D. C. Effects of dielectric saturation upon the diffuse double layer and the free energy of hydration of ions. *J. Chem. Phys.* **1950**, *18*, 903−909. (b) Kornyshev, A. A.; Sutmann, G. Nonlocal dielectric saturation in liquid water. *Phys. Rev. Lett.* **1997**, *79*, 3435−3438.
(42) (a) Wang, C.; Danovich, D.; Chen, H.; Shaik, S. Oriented External Electric Fields: Tweezers and Catalysts for Reactivity in Halogen-Bond Complexes. *J. Am. Chem. Soc.* **2019**, *141*, 7122−7136. (b) Friedrich, B.; Herschbach, D. R. Spatial orientation of molecules in strong electric fields and evidence for pendular states. *Nature* **1991**, *353*, 412. Friedrich, B.; Herschbach, D. Enhanced orientation of polar molecules by combined electrostatic and nonresonant induced dipole forces. *J. Chem. Phys.* **1999**, *111*, 6157−6160.
(43) The contribution of additional layers of solvent can be expected to decrease rapidly as the thickness of the reaction medium grows due to the inverse square dependence of Coulomb's law of the distance.

https://dx.doi.org/10.1021/jacs.9b13029
J. Am. Chem. Soc. 2020, 142, 9955−9965